

Submitted 11th March 2008

Supernova Shock Breakout from a Red Supergiant

Kevin Schawinski,^{1*} Stephen Justham,^{1*} Christian Wolf,^{1*} Philipp Podsiadlowski,¹ Mark Sullivan,¹ Katrien C. Steenbrugge,² Tony Bell,¹ Hermann-Josef Röser,³ Emma Walker,¹ Pierre Astier,⁴ Dave Balam,⁵ Christophe Balland,⁴ Stephane Basa,⁶ Ray Carlberg,⁷ Alex Conley,⁷ Dominique Fouchez,⁸ Julien Guy,⁴ Delphine Hardin,⁴ Isobel Hook,¹ Andy Howell,⁷ Reynald Pain,⁴ Kathy Perrett,⁷ Chris Pritchett,⁵ Nicolas Regnault⁴ and Sukyoung K. Yi⁹

ABSTRACT

Massive stars undergo a violent death when the supply of nuclear fuel in their cores is exhausted, resulting in a catastrophic ‘core-collapse’ supernova. Such events are usually detected long after the star has exploded. Here we report the first detection of the radiative precursor from a supernova shock before it has reached the surface of a star followed by the initial expansion of the star at the beginning of the explosion. Theoretical models of the ultraviolet light curve show that the progenitor was a red supergiant, as expected for this type of supernova. These observations provide a promising and novel way to probe the physics of core-collapse supernovae and the internal structures of their progenitors.

The explosive deaths of massive stars are dramatic events which seed the Universe with heavy elements (1, 2), produce black holes, pulsars and the most energetic gamma-ray bursts (GRBs; 3), whilst their energy input can regulate the growth of galaxies (4). Even though a large amount of theoretical effort has been expended on trying to explain how the terminal collapse of a star’s

¹Department of Physics, University of Oxford, Oxford OX1 3RH, UK.

²St John’s College Research Centre, University of Oxford, OX1 3JP, UK.

³Max-Planck-Institut für Astronomie, Königstuhl 17, 69117 Heidelberg, Germany.

⁴LPHNE, CNRS-IN2P3 and Universités Paris VI & VII, 4 Place Jussieu, 75252 Paris Cedex 05, France.

⁵Department of Physics and Astronomy, University of Victoria, PO Box 3055 STN CSC, Victoria, BC V8T 3P6, Canada.

⁶LAM, CNRS, BP8, Traverse du Siphon, 13376 Marseille Cedex 12, France.

⁷Department of Physics and Astronomy, University of Toronto, 50 St. George Street, Toronto, ON M5S 3H4, Canada.

⁸CPPM, CNRS-IN2P3 and Universit Aix-Marseille II, Case 907, 13288 Marseille Cedex 9, France.

⁹Department of Astronomy, Yonsei University, Seoul 120-749, Korea.

* email: kevin@astro.ox.ac.uk, sjustham@astro.ox.ac.uk, cwolf@astro.ox.ac.uk

core leads to a luminous supernova, we still do not fully understand the process by which the collapse of the core produces an outward-moving shock that leads to the ejection of the envelope (5–7). This shock heats and accelerates the stellar envelope as it passes through it. By the time the shock dissipates at the surface of the star, several solar masses of previously static envelope material are expanding at several percent of the speed of light. At the time of core collapse, a nearby external observer equipped with a detector of neutrinos or of gravitational waves might receive a brief warning of the future explosion, but for most of the passage of the shock through the star that observer would notice no further change. Only when the shock approaches the surface does radiation diffuse far enough ahead of the shock wave to raise the temperature of the stellar photosphere. This phase is sometimes referred to as ‘shock breakout’, although the associated radiation is due to the ‘radiative precursor’ of the shock, long before the shock actually reaches the surface. This radiative precursor raises the temperature of the star to $\sim 10^5$ K before the surface expands dramatically (8).

There have been some previous claims of observations of shock breakouts, usually in the context of relatively local GRBs and X-ray flashes, and involving shocks traveling through dense winds *outside* compact blue stars that have previously been stripped of their hydrogen envelopes, not shocks emerging from the surface of the stars themselves (9, 10). Moreover, these claims have been disputed (11–14). Here we present the first data that unambiguously show the brightening of a red supergiant due to the theoretically predicted radiative precursor *before the supernova shock reaches the surface* of the star. Such observations do not only provide valuable information about the density profile inside the progenitor star (15) and the physics of radiative shocks, but knowledge of the spectrum of the associated ultraviolet flash has important implications for the ionization of the circumstellar medium (16, 17).

Although core-collapse supernovae are expected to be most luminous around the time of shock breakout, most of this energy emerges as extreme UV or soft X-ray radiation. Hence core-collapse supernovae are typically only discovered several days after the SN explosion near the peak of their optical light curve; observations of early light curves are rare (18, 19). To circumvent this problem, we exploit two complementary data sets: an optical survey to locate SNe, and UV data to search for serendipitously associated shock breakouts. The first is the Supernova Legacy Survey (SNLS; 20), which studies distant supernovae using data taken every 4 days at the 3.6 m Canada-France-Hawaii Telescope (CFHT). The second is from the *GALEX* ultraviolet space telescope (21, 22), which took a deep 100 hour combined exposure coincident with the early-2004 SNLS data in the “COSMOS” survey field (23, 24). The *GALEX* data were taken using sub-exposures of 15 to 30 minutes over the course of several weeks, providing data with the time resolution necessary to resolve UV-luminous events occurring prior to the SNLS supernovae.

One SNLS event, designated SNLS-04D2dc and confirmed as a Type II supernova from an optical spectrum taken at the ESO Very Large Telescope (see appendices), shows a dramatic brightening in the *GALEX* near-UV images about two weeks prior to discovery by the SNLS, consistent with shock breakout. The host galaxy appears to be a normal star-forming spiral galaxy at a redshift of

$z = 0.1854$. We present the supernova spectrum, Gemini host galaxy spectrum and *Hubble Space Telescope* image of the host in the supplementary online material. Fig. 1 shows the SNLS optical and *GALEX* UV light curves of this supernova together with the *GALEX* near-UV images at various phases. The “plateau” in the optical light curve identifies it as a type IIP supernova (see Fig. 1), implying a red-supergiant progenitor (25, 26). Due to bad weather and technical problems with the CFHT camera, there are no optical data concurrent with the UV; however, *GALEX* observed the entire radiative precursor. Fig. 2 shows a detailed enlargement of the UV light curve during the event.

The *GALEX* light curve is unique in that it probes the arrival of the supernova shock at the surface of the star. We can interpret this light curve as follows. The first peak in the light curve is due to radiation traveling ahead of the shock wave. This heats the surface of the star before it begins to explode. The near-UV light curve samples the brightening caused by this precursor over approximately 6 hours. The gas temperature inside the shock is lower than the radiation temperature produced at the shock front itself. This causes a drop in the luminosity of the star after the radiative precursor has escaped (8). The near-UV light curve in Fig. 2 clearly shows this dip in luminosity, dropping almost to the background level of UV emission from the host galaxy.

We can compare the duration of the observed precursor with theoretical expectations by equating the photon diffusion time-scale with the time-scale for the shock to escape from the envelope. If v is the shock speed and the density of the hydrogen-dominated atmosphere is ρ , we find $d \approx 2.5 \times 10^{11} \text{ m}(10^{-8} \text{ kg m}^{-3}/\rho)(10^7 \text{ m s}^{-1}/v)$ for the depth of the shock d (from the surface of the star) at the time when the radiative precursor becomes visible at the surface (for details see the appendices). This value for d leads to a prediction for the duration of the shock precursor of $d/v = 2.5 \times 10^4 \text{ s}$ for the parameters above, i.e. almost 7 hours, remarkably consistent with our observations of the precursor. This indicates that the progenitor was a very large star, i.e. a red supergiant, as expected for the progenitor of a type IIP supernova (25, 26). In order to model the radiative precursor, we have solved simplified radiation-hydrodynamics equations for an outward-moving shock inside a stellar envelope. Fig. 3 shows representative models that are consistent with the data; again they require radii and envelope densities appropriate for a red-supergiant star. More detailed future observations of the shock breakouts from local supernovae should help to constrain, for example, the structure of each star’s outer envelope. More sophisticated modelling will be required to fully exploit future data (8, 27).

Although the radiative precursor does cause some moderate expansion of the star, there is little change in the stellar radius until the shock reaches the surface. During the early stages of the subsequent explosive expansion of the star, the radiation-dominated plasma in the envelope continues to cool, primarily due to adiabatic expansion at almost constant velocity (1). Since the physics that dominates the light curve during this adiabatic phase is relatively well understood, our modeling of this phase is comparatively robust. The photospheric temperature T is inversely proportional to the photospheric radius R , hence the total luminosity L of the supernova continues to drop: the decrease due to the Stefan-Boltzmann law ($L \propto T^4 \propto R^{-4}$) is greater than the

increase due to the growing surface area ($L \propto R^2$). However, the observed UV luminosity initially increases even though the bolometric luminosity drops, because the peak in the spectral energy distribution moves across the *GALEX* UV bands. The model curves in Fig. 2 shows that this simple physical description reproduces the *GALEX* data with parameters as expected for a red supergiant progenitor. Initial photospheric radii of 500–1000 R_\odot , expansion velocities of $1\text{--}2 \times 10^7 \text{ m s}^{-1}$ and initial temperatures of $\sim 10^5 \text{ K}$ match the observed fluxes very well. The biggest uncertainty in these values arises from the uncertainty in the adopted extinction (see appendices); any increase in the NUV extinction would increase the range of preferred initial radii.

In summary, we have for the first time detected the radiative precursor of a supernova shock, probing the propagation of a supernova shock inside a red supergiant’s envelope. We have also observed the very early stages of the explosive expansion of that star. This unique discovery has only been possible by combining data from SNLS ground-based observations with *GALEX* UV data. We encourage coordinated searches linking space-based UV observatories with optical supernova surveys. Our predicted rates for events that can be detected by *GALEX* show that a dedicated search for similar events is likely to yield more examples. These will allow us to systematically study the internal structures of red-supergiant envelopes and the properties of supernova shock waves and to probe the ‘first light’ of supernovae, a phase that until now had been inaccessible.

REFERENCES

- (1) D. Arnett, *Supernovae and nucleosynthesis. An investigation of the history of matter, from the Big Bang to the present* (Princeton series in astrophysics, Princeton, NJ: Princeton University Press, 1996).
- (2) K. Nomoto, N. Tominaga, H. Umeda, C. Kobayashi, K. Maeda, *Nuclear Physics A* **777**, 424 (2006).
- (3) C. L. Fryer, *et al.*, *PASP* **119**, 1211 (2007).
- (4) A. Dekel, J. Silk, *ApJ* **303**, 39 (1986).
- (5) R. Buras, M. Rampp, H.-T. Janka, K. Kifonidis, *Physical Review Letters* **90**, 241101 (2003).
- (6) A. Mezzacappa, *Ann. Rev. Nucl. Part. Sci.* **55**, 467 (2005).
- (7) A. Burrows, E. Livne, L. Dessart, C. D. Ott, J. Murphy, *ApJ* **640**, 878 (2006).
- (8) L. Ensmann, A. Burrows, *ApJ* **393**, 742 (1992).
- (9) S. Campana, *et al.*, *Nature* **442**, 1008 (2006).
- (10) A. M. Soderberg, *et al.*, *ArXiv:802:1712* (2008).
- (11) P. A. Mazzali, *et al.*, *Nature* **442**, 1018 (2006).

- (12) L.-X. Li, *MNRAS* **375**, 240 (2007).
- (13) G. Ghisellini, G. Ghirlanda, F. Tavecchio, *MNRAS* **382**, L77 (2007).
- (14) L.-X. Li, *arXiv:0803.0079* (2008).
- (15) A. J. Calzavara, C. D. Matzner, *MNRAS* **351**, 694 (2004).
- (16) C. Fransson, P. Lundqvist, *ApJ* **341**, L59 (1989)
- (17) P. Lundqvist, *ApJ* **511**, 389 (1999)
- (18) M. Stritzinger, *et al.*, *AJ* **124**, 2100 (2002).
- (19) R. M. Quimby, *et al.*, *ApJ* **666**, 1093 (2007).
- (20) P. Astier, *et al.*, *A&A* **447**, 31 (2006).
- (21) D. C. Martin, *et al.*, *ApJ* **619**, L1 (2005).
- (22) P. Morrissey, *et al.*, *ApJS* **173**, 682 (2007).
- (23) N. Scoville, *et al.*, *ApJS* **172**, 1 (2007).
- (24) M. A. Zamojski, *et al.*, *ApJS* **172**, 468 (2007).
- (25) S. W. Falk, W. D. Arnett, *ApJ* **180**, L65 (1973).
- (26) S. J. Smartt, *et al.*, *Science* **303**, 499 (2004).
- (27) R. A. Chevalier, R. I. Klein, *ApJ* **234**, 597, (1979).

Acknowledgements

KS is supported by the Henry Skynner Junior Research Fellowship at Balliol College, Oxford. SJ acknowledges support by STFC & Global Jet Watch, CW and ESW by STFC and MS by the Royal Society. *GALEX* (*Galaxy Evolution Explorer*) is a NASA Small Explorer, launched in 2003 April. We gratefully acknowledge NASA’s support for construction, operation, and science analysis for the *GALEX* mission, developed in cooperation with the Centre National d’Etudes Spatiales of France and the Korean Ministry of Science and Technology. This paper is based in part on observations obtained with MegaPrime/MegaCam, a joint project of CFHT and CEA/DAPNIA, at the Canada-France-Hawaii Telescope (CFHT) which is operated by the National Research Council (NRC) of Canada, the Institut National des Sciences de l’Univers of the Centre National de la

Recherche Scientifique (CNRS) of France, and the University of Hawaii. This work is based in part on data products produced at the Canadian Astronomy Data Centre as part of the CFHT Legacy Survey, a collaborative project of NRC and CNRS. Based on observations obtained at the European Southern Observatory using the Very Large Telescope on the Cerro Paranal (ESO Large Programme 171.A-0486). Based on observations obtained at the Gemini Observatory (program number GN-2007B-Q17), which is operated by the Association of Universities for Research in Astronomy, Inc., under a cooperative agreement with the NSF on behalf of the Gemini partnership: the National Science Foundation (United States), the Science and Technology Facilities Council (United Kingdom), the National Research Council (Canada), CONICYT (Chile), the Australian Research Council (Australia), Ministério da Ciência e Tecnologia (Brazil) and SECYT (Argentina). We also thank the COSMOS team for their efforts.

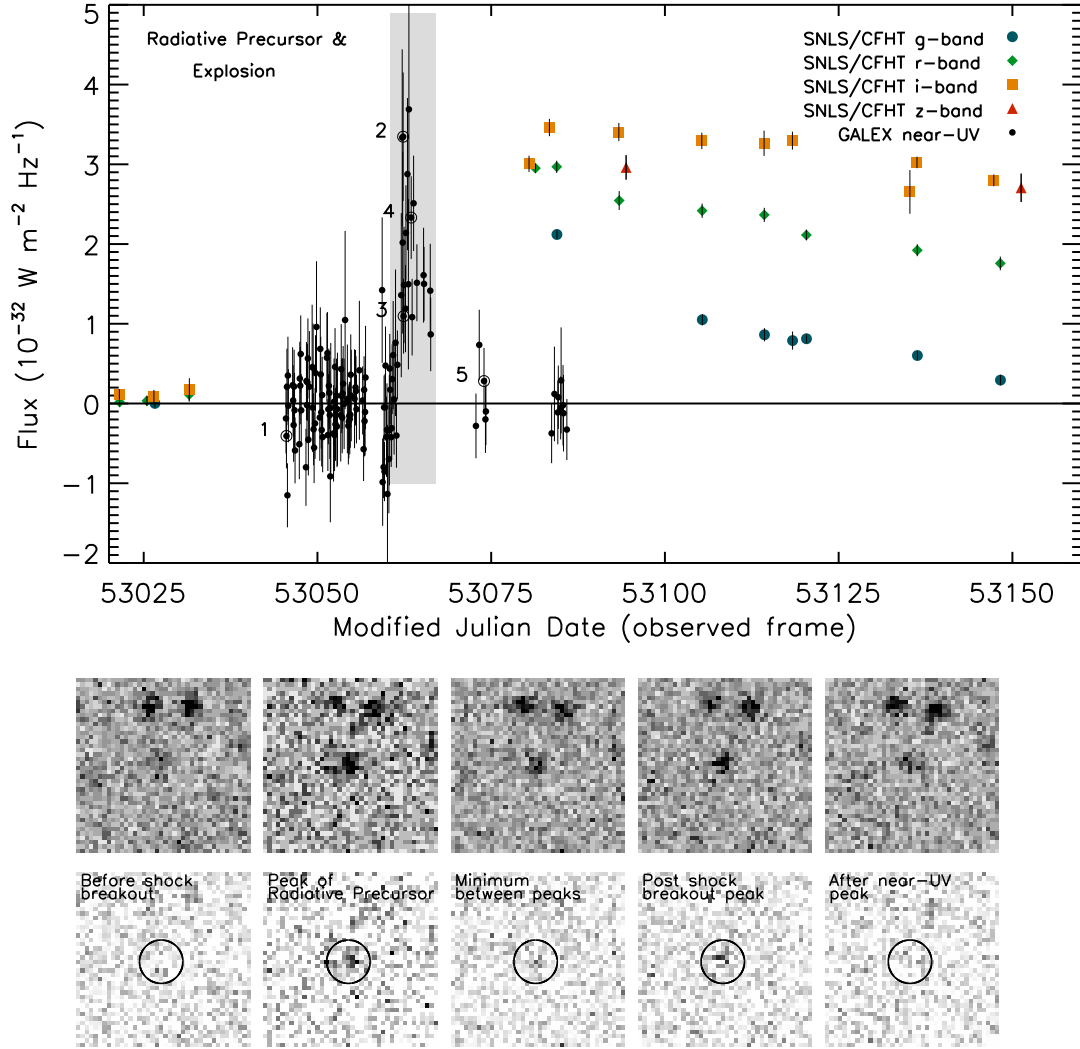


Fig. 1. Composite of the optical SNLS and the UV *GALEX* light curves, i.e. observed fluxes as a function of modified Julian date. All fluxes are host galaxy subtracted and are not corrected for internal extinction. The gray box indicates the time of the radiative precursor. The points highlighted by circles indicate five phases of the radiative precursor in the UV, as observed by *GALEX*. These five phases are illustrated by a time sequence of original near-UV images (upper row, 1×1 arcmin) and difference images (lower row, with a pre-SN image subtracted) to emphasize the transient source. The lack of optical data during the UV event is due to both poor weather conditions and technical problems.

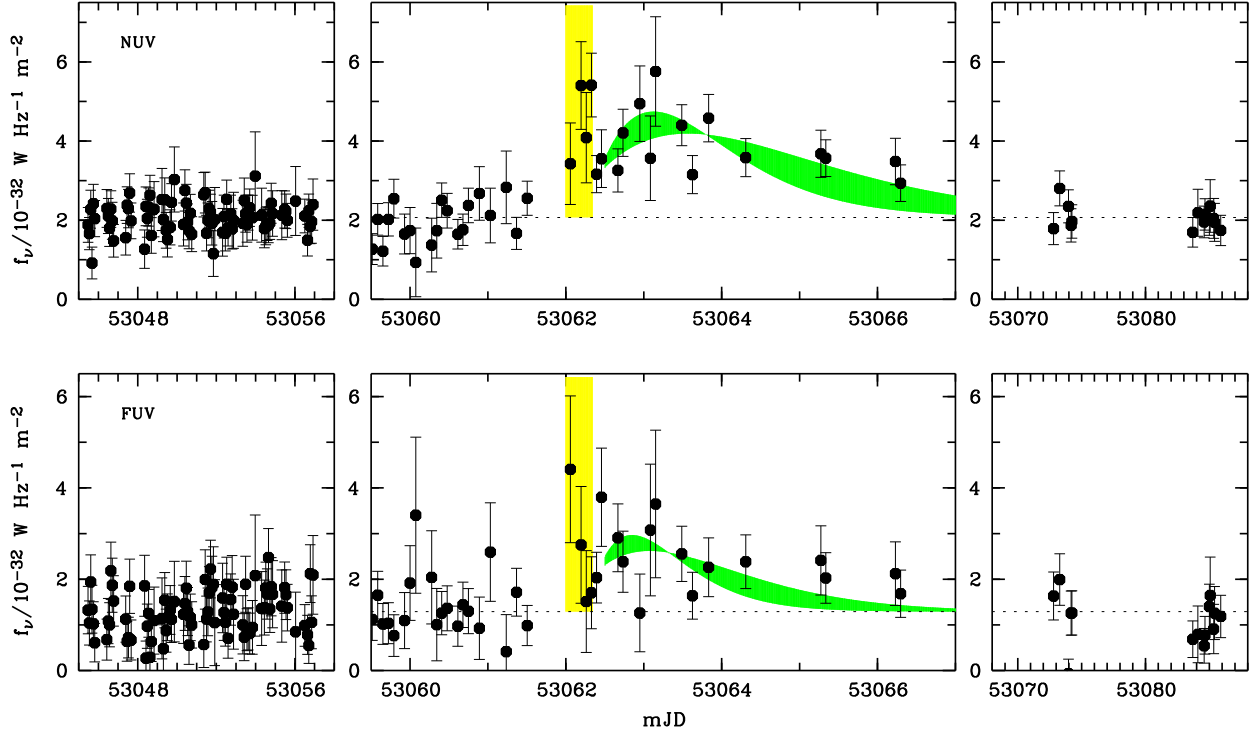


Fig. 2. The *GALEX* near-UV and far-UV flux against time (modified Julian date in days). This is a zoomed-in version of the shaded time range of Fig. 1. The background levels are shown before and after the supernova (left and right panels), and the central panels show the event itself. The radiative precursor is highlighted in yellow. Models for the post-explosion expansion are shaded in green; these models assume an initial photospheric radius of 500–1000 R_\odot . The width of the green band is due to the range of assumed expansion velocities ($1 - 2 \times 10^7 \text{ m s}^{-1}$). These models assume adiabatic free expansion of a radiation-dominated plasma and black-body emission from a well-defined photosphere (see text). The models were only fitted to the NUV data, but are also consistent with the FUV data.

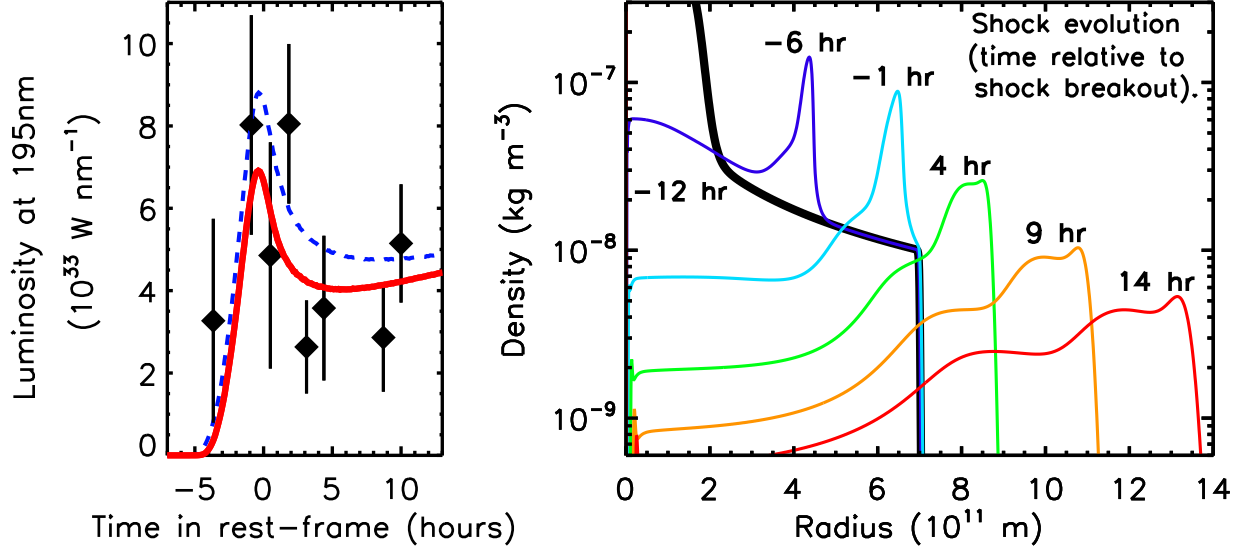


Fig. 3. *Left panel:* representative model precursor light curves compared to the precursor data (diamonds with error bars). The solid red curve represents the light curve produced from a model with an initial radius of $7 \times 10^{11} \text{ m}$ ($\approx 1000R_{\odot}$) and an initial density distribution $\propto 1/r$. The dashed curve in the left hand panel shows an identical model except that the initial radius was 10^{12} m ; the absolute normalisation of these luminosities is uncertain to factors of order unity (see appendices for details). The zero-point of the time axis is approximately at shock breakout. *Right panel:* the time evolution of the internal density profile for the model producing the *solid* light curve in the left panel. Around 4 hours before the shock has reached the surface the UV luminosity has already begun to rise.

Appendices

A1 Spectra of Supernova and Host Galaxy

SNLS searches for high-redshift supernovae (SNe) with the goal of measuring about 500 distant Type Ia supernovae (SNe Ia) for use in studying dark energy. The volume and depth of these observations also allows detection of a large number of core-collapse SNe. While the dedicated spectroscopic follow-up of SNLS is prioritised for the SN Ia candidates, a spectrum for 04D2dc (located at RA = 10:00:16.7, Dec = +02:12:18.52, J2000) was obtained a few days after discovery at the European Southern Observatory Very Large Telescope.¹ The spectrum provided an excellent match to a type II SN (Fig. A1) located in a star-forming galaxy at a redshift $z = 0.1854$. A second spectrum obtained in early 2008 at the Gillett Gemini North Telescope after the SN had faded confirms the presence of strong emission lines in the spiral host galaxy. In Figs. A1 and A2, respectively, we present the spectra and the *Hubble Space Telescope* F814W image of the host galaxy from the COSMOS survey.

We have extracted a spectrum at the location of the SN inside the galaxy to estimate the host galaxy extinction based on the Balmer decrement of the galaxy spectrum. We used the SMC reddening law (A1) to estimate the extinction in the GALEX bands, which is appropriate for most star-forming galaxies at most redshifts including lower-mass galaxies at low redshift. The colour excess E_{B-V} was determined from the Balmer decrement at the location of the SN and gives an implied extinction on the GALEX UV filters of $A_{\text{NUV}} = 1.45$ mag and $A_{\text{FUV}} = 2.39$ mag. The largest source of uncertainty in the extinction measurement is probably its low spatial resolution. From the variation in E_{B-V} we see between stars within ~ 1 kpc of the Sun, we estimate that the uncertainty in the absolute extinction of the supernova could be as much as a factor of two.

A2 GALEX Data Reduction

We determined the photometry for the NUV light curve by processing image frames of $10' \times 10'$ size centered on the SN using the MPIAPHOT package (A2). We co-added a selection of 161 frames with a reasonably Gaussian PSF to obtain best-possible position estimates when searching objects with SExtractor (A3). We then transformed the coordinates of the object list back into the coordinate frames of each single exposure and measured fluxes centered on the projected object positions.

We suppressed the propagation of variations in the PSF (presumably mostly due to focus

¹ESO/VLT large programme number 171.A-0486.

drifts) into the photometry by making sure that we always probe the same physical footprint $f(x, y)$ of any object in all exposures irrespective of the PSF $p(x, y)$. Here, the footprint $f(x, y)$ is the convolution of the PSF $p(x, y)$ with the aperture weighting function $a(x, y)$. If all three are Gaussians, an identical physical footprint can be probed even when the PSF changes, simply by adjusting the weighting function $a(x, y)$ for each frame. We chose to measure fluxes on a footprint of 7.5" FWHM, so that on average $p \approx a$, which optimizes the signal-to-noise ratio of point sources.

Hence, we measure the PSF on each individual frame, choose the weighting function needed to conserve the footprint and obtain the flux on the footprint. Individual frames are normalized to each other using the count rates of the 15 brightest non-variable objects. Fluxes from individual frames are averaged for each object and the flux error is derived from the scatter. Thus, it takes not only photon noise into account, but also sub-optimal flat-fielding, errors in the background determination and uncorrected detector artifacts. All fluxes are finally calibrated to the GALEX photometric catalogues using the brightest stars. As such the MPIAPHOT aperture fluxes correspond to total fluxes for point sources, but underestimate them for extended sources. In this way, we have measured the NUV flux from the SN alone (the excess flux over the host level) in a physically non-variable aperture, with ideal S/N, and correctly calibrated.

Fig. A3 shows the distribution of NUV object flux scatter vs. mean fluxes for ~ 1000 objects detected in the selected area. Only two objects, the SN and a QSO, appear as significantly variable by showing more flux scatter among the frames than expected from Poissonian noise. When sources are fainter than the background, their flux scatter is driven by constant noise in the estimated background (horizontal arm). The scatter of bright sources is dominated by Poisson fluctuations in the source flux, so these form a steep arm at slope 1/2 (in a log-log plot).

Fig. 2 shows part of the resulting light curve; a large group of frames obtained two years after the SN event is omitted as it shows just the host galaxy light at the same level and scatter as before the event.

The FUV images have been processed in a similar fashion except that the low count rates are a challenge for determining the PSF, background and normalization of individual frames. The resulting FUV fluxes should be considered uncertain at a $\pm 30\%$ level in each frame. For this reason the FUV light curve is only shown to indicate that excess fluxes are observed exactly at the time of the NUV event, but the FUV data are not included in the model fit for the photospheric expansion. The model curves are plotted in the FUV panels just as they are predicted by the NUV fit.

A3 Analytic Estimates for the Radiative Precursor

Here we give more details about the derivation of the scaling relations given in the main text.

A3.1 Estimated Depth and Duration

First we estimate the depth of the shock d within the star at the start of the radiative precursor. This is defined by equating the photon diffusion time-scale τ_{diff} with the time-scale for the shock to escape τ_s , where

$$\tau_{\text{diff}} \approx \frac{3d^2}{\alpha l c}, \quad (1)$$

$$\tau_s \approx \frac{d}{v}, \quad (2)$$

and l is the photon mean free path, v is the shock speed, c is the speed of light and α is a constant which depends on the density profile of the progenitor (1). The value of α is ≈ 10 for a uniform density sphere or ≈ 30 or ≈ 90 if the density profile of the sphere drops as r^{-1} or r^{-2} , respectively. If the system is better modeled by a thin shell than a uniform sphere, then $\alpha = 1$. Our assumption of $\alpha \approx 10$ and of a roughly constant density in the relevant part of the envelope seems reasonable.

Equating τ_{diff} with τ_s and rearranging produces

$$d \approx \frac{\alpha c l}{3v} \quad (3)$$

in which we will substitute the mean free path for an opacity κ dominated by electron scattering in a hydrogen atmosphere $\kappa_{\text{es,H}}$ of density ρ . This gives:

$$d \approx 2.5 \times 10^{11} \text{ m} \left(\frac{\alpha}{10} \right) \left(\frac{\kappa}{\kappa_{\text{es,H}}} \right)^{-1} \left(\frac{\rho}{10^{-8} \text{ kg m}^{-3}} \right)^{-1} \left(\frac{v}{10^7 \text{ m s}^{-1}} \right)^{-1} \quad (4)$$

for the depth of the shock at the time when the radiative precursor becomes visible at the surface. In the main text, we have omitted the dependence on α and κ for simplicity. Note that the depth estimated here is a very good match to the depth of the shock in Fig 3. at the start of the radiative precursor.

This value for d is $\sim 350 R_\odot$. As the progenitor's radius must be larger than d , we require a red supergiant, as expected for a IIP SN. The duration of the radiative precursor should be $d/v = 2.5 \times 10^4 \text{ s}$ for the parameters above, i.e. almost 7 hours and thus in good agreement with our observations. To be precise, we should increase this duration by the light travel time across the disc, but this constitutes a fairly small correction.

The density adopted here is consistent with the envelopes of red-supergiant models used in previous SN modeling (A4).

A3.2 Estimated Energy Release

We can estimate the total energy released in the radiative precursor E_{rp} in a way almost independent of the density profile. The total energy radiated during the passage of a radiation-dominated shock with velocity v through a mass M is $\approx (18/49)Mv^2$ and we can approximate the

mass as $M \approx 4\pi R^2 \rho d$, where ρ and d are again the density of the outer envelope and the depth of the shock when the radiative precursor is first visible. We take R to be the radius of the star, which is a good approximation if $R \gg d$. We can now replace d using Eq. (A2) and then use $\rho l = \kappa^{-1}$ to obtain

$$E_{rp} \approx \left(\frac{18}{49}\right) 4\pi R^2 \frac{\alpha c v}{3\kappa}, \quad (5)$$

$$E_{rp} \approx 2.3 \times 10^{42} \text{ J} \left(\frac{R}{10^{12} \text{ m}}\right)^2 \left(\frac{\alpha}{10}\right) \left(\frac{v}{10^7 \text{ m s}^{-1}}\right)^{-1} \left(\frac{\kappa}{\kappa_{\text{es,H}}}\right)^{-1}. \quad (6)$$

Dividing this by a duration of $\sim 10^4$ s predicts a mean luminosity of $\sim 10^{38}$ W, consistent with our extrapolation from the observed UV flux using a temperature of $\sim 10^5$ K (see section A4.2).

A4 Numerical Light Curve Models

We have produced UV light curves for both the radiative precursor and the post-shock-breakout adiabatic expansion. Our simple numerical models use the physics essential to the respective phases. They naturally produce light curves consistent with the data using the expected physical input and the very minimum of parameter fitting.

The following models both produce a spectral energy distribution (SED). The effects of cosmological redshift were applied to the SED and the time axis of the expansion. The full *GALEX* filter functions were used to define the NUV and FUV bands. The extinction of the UV emission probably constitutes the biggest uncertainty in our models. We have used measured values for the extinction (see section A1) such that the NUV flux which reaches us is $\approx 1/3.8$ of the emitted flux, and the FUV flux is $\approx 1/9.0$ of the unextinguished value. However, even the ‘local’ measurements of the host galaxy’s extinction are not guaranteed to be exactly the same as those which would be appropriate for the SN (see section A1).

A4.1 The Radiative Precursor

To model the radiative precursor we have written a bespoke one-dimensional hydrodynamic code. The code is Eulerian; we have used 800 radial cells across the initial model (hence with a typical cell size of $\sim 10^9$ m) and 4000 cells in total. Radiation transport is handled during each timestep by solving the diffusion equation for the internal energy U within the moving radiation-dominated plasma, where the diffusion constant is $c/(3\rho\kappa)$ and we assume that the opacity κ is mostly due to electron scattering inside a hydrogen-dominated plasma. In addition to elastic Compton scattering, the radiation treatment includes Compton cooling and bremsstrahlung (A5), and the hydrodynamics naturally incorporates advection and adiabatic cooling. When a temperature is required for the emission model we take the fourth root of the energy density, $T = (cU/4\sigma)^{(1/4)}$.

The initial conditions specify a density distribution for the cold (10 eV) envelope and for the hot (1 MeV) core. The core properties were chosen such as to eventually produce a shock moving with a characteristic velocity of $1 - 2 \times 10^7 \text{ m s}^{-1}$. Note that this means that the first model in Fig. 3 is not at core collapse, or directly taken from a stellar evolution code. The times in Fig. 3 are approximately relative to shock breakout.

This model includes the essential physics to describe the motion of the shock through the star. However, modelling the exact spectral energy distribution and luminosity of the radiative precursor would be a much more complex task, partly as during shock breakout the luminosity may be augmented by some non-thermal emission (A6). To the accuracy currently demanded by the data in the UV waveband, it seems reasonable to approximate the emission as black-body.

We do not attempt a full solution of the radiative-transfer problem, but note that the photons which have diffused to the surface will carry a temperature which was imprinted on them deeper in the star, as the opacity is largely due to elastic scattering from electrons. We estimate that the typical photon will have diffused from an optical depth of $c/3v_{\text{shock}}$ and therefore adopt this depth to define the characteristic temperature for the black body. However, the radiation flux at the surface will be somewhat lower than at the optical depth where the photons originated (as the diffusion speed is rather lower than the speed of light). Our models indicate that the intensity of emission will be lower by up to a factor of five than would be expected for this black-body temperature over the entire surface. Given those uncertainties, the light curves in Fig. 3 have been roughly rescaled down to show that expected shapes are consistent with the data. The solid light curve in Fig. 3 has been multiplied by 1/2.5 and the dashed by 1/4, both within the uncertainties of this modelling.

In addition to any simplifications introduced in our modelling, we note that most of the luminosity during the radiative precursor will be emitted at higher energies than we directly observe; it is unclear whether a significant fraction of those shorter-wavelength photons will lead to the production of UV radiation through some indirect route.

This model has the significant benefit of physical clarity, but more detailed and complex work will be needed to fully exploit future observations.

A4.2 After Shock-Breakout

After the radiative precursor, *GALEX* has observed the early stages of the SN’s expansion. As summarized in the main text, this phase is relatively simple to understand. The radiation-dominated plasma expands freely (with almost constant velocity) and cools adiabatically, hence $T \propto 1/R$ (A7). The energy source is the internal energy of the plasma; radioactivity is only relevant much later. Our model also assumes that the emission can be approximated by a single-temperature black body, and this rest-frame SED is converted into an observer-frame *GALEX* UV flux as described at the start of section A4. The assumption that there is a well-defined photosphere

is reasonable for the very early stages of expansion which we have observed.

The model light curves represented in Fig. 2 were produced by this physical model of free adiabatic expansion. The initial radius and expansion velocity were set by hand to a range of expected values for the progenitor of such a type IIP SNe. Then the initial temperature and time of explosion were fitted such that the χ^2 parameter with respect to the NUV data was minimized. The FUV data was not fitted, but the model light curves are still consistent with the data. This second phase, visible in the UV after the radiative precursor, constrains the dimensions of the precursor independently of the precursor model.

As the envelope cools and becomes less dense, the later behavior and definition of the photosphere is more complex. In particular, the plateau in the late-time optical light curve that is characteristic of type IIP SNe is thought to be due to such complications. During the plateau, the effective photosphere moves inwards in mass but remains at an almost constant radial position and temperature. The color of the SN is not precisely constant during the plateau (see Fig. 1); the emission during that stage is not from a simple black body.

There seems to be some confusion over whether the observations in (A8) have resolved shock breakout in the type Ib/c SN 1999ex. The progenitor of 1999ex would not be a red supergiant but a much more compact star. Note that the cadence of their observations is easily long enough to miss the radiative precursor that we have observed. The timescale of the early dip they observe in the U band is consistent with the timescale we find for the early phase of adiabatic cooling. We thus find it extremely unlikely that (A8) observed the shock emerging from within the star.

A5 Suggestions for Further Observations

Finding more events like 04D2dc will help further our understanding of core-collapse SNe. We provide some general ideas on how a larger sample of such events might be obtained. The starting place for any such survey design must be the assumption that 04D2dc was a normal event; we assume that a UV light curve of the same absolute magnitude in the near-UV is associated with all – or at least a majority of – Type II SNe. If this is the case, we must further consider the dust extinction in the host galaxies and the locations of Type II SNe. The near-UV is much more sensitive to dust extinction than optical wavelengths and so it is conceivable that a SN Type II occurring in a heavily extincted host galaxy is detected in optical filters, but remains undetected in the UV.

Taking our discovery of 04D2dc as the starting point, we can estimate the rate of such events in a SN survey similar to SNLS. 04D2dc is at the edge of what is detectable in single *GALEX* visits, so we can expect that no similar events will be detectable beyond a redshift of $z \sim 0.2$ (the host galaxy of 04D2dc is at $z = 0.1854$). We can compute the expected SN Type II rate from the typical cosmic star formation density out to $z \sim 0.2$ probed by one *GALEX* field of view (circular, 1.4 deg diameter). The co-moving volume probed by this field of view is $\sim 8 \times 10^4$ Mpc³. Combining this

with a star formation rate density of $\rho_{\text{SFR}} \sim 0.03 \text{ M}_{\odot}\text{yr}^{-1}\text{Mpc}^{-3}$ (A9) yields a total star formation rate probed of $\sim 2.5 \times 10^3 \text{ M}_{\odot}\text{yr}^{-1}$. Assuming a core-collapse rate of 1 per century per $4\text{M}_{\odot}\text{yr}^{-1}$, this results in 6.2 events per year per field of view. There are of course substantial uncertainties in this estimate.

Thus, mounting a substantial *GALEX* observational effort covering e.g 4 fields-of-view continuously would yield about 2 such events per month. A dedicated optical photometry and spectroscopic survey for prompt follow-up of any detected events would also be necessary. The resulting deep *GALEX* image will also be scientifically useful for other purposes. The key feature of any future similar observations must remain the high cadence. *GALEX* with its ultraviolet capability and orbit is the most suitable platform for further research into the radiative precursors of supernovae.

References and Notes

- A1. Y. C. Pei, *ApJ* **395** 130 (1992).
- A2. H.-J. Röser, K. Meisenheimer, *A&A* **252**, 458 (1991).
- A3. E. Bertin, S. Arnouts, *A&AS* **117**, 393 (1996).
- A4. S. W. Falk, W. D. Arnett, *ApJS* **33**, 515 (1977).
- A5. R. A. Chevalier, R. I. Klein, *ApJ* **234**, 597, (1979).
- A6. R. I. Klein, R. A. Chevalier, *ApJ* **223**, L109 (1978).
- A7. D. Arnett *Supernovae and nucleosynthesis. An investigation of the history of matter, from the Big Bang to the present* Princeton University Press (1996)
- A8. M. Stritzinger, *et al.*, *AJ* **124**, 2100 (2002).
- A9. K. Glazebrook, *et al.*, *ApJ* **587**, 55 (2003).

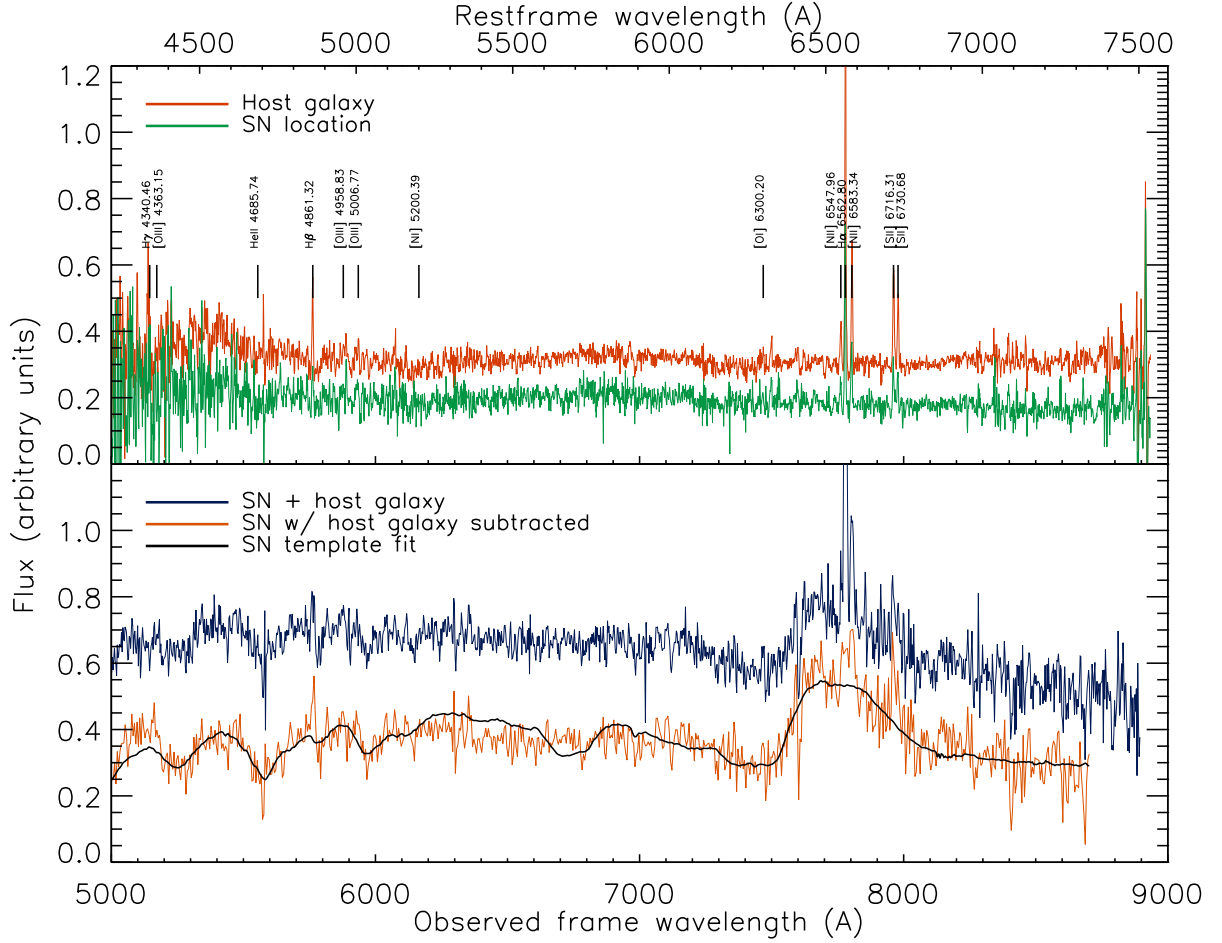


Fig. A1. In the upper panel, we show the Gemini spectra of the host galaxy as a whole and of the SN location. Both show strong emission lines as expected of a spiral galaxy, including $H\alpha$ and $H\beta$ from which we estimate the extinction affecting the SN. In the lower panel we show the VLT spectrum of the SN, prior to and after the subtraction of a host galaxy template, together with an SN Type IIP template identifying the SN type.

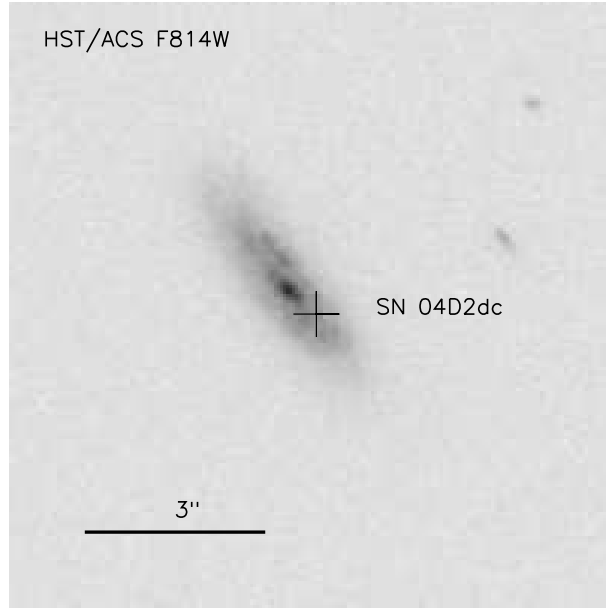


Fig. A2. The *Hubble Space Telescope* F814W-band image of the host galaxy from the COSMOS survey. We indicate the position of the SN and the image scale in arcseconds.

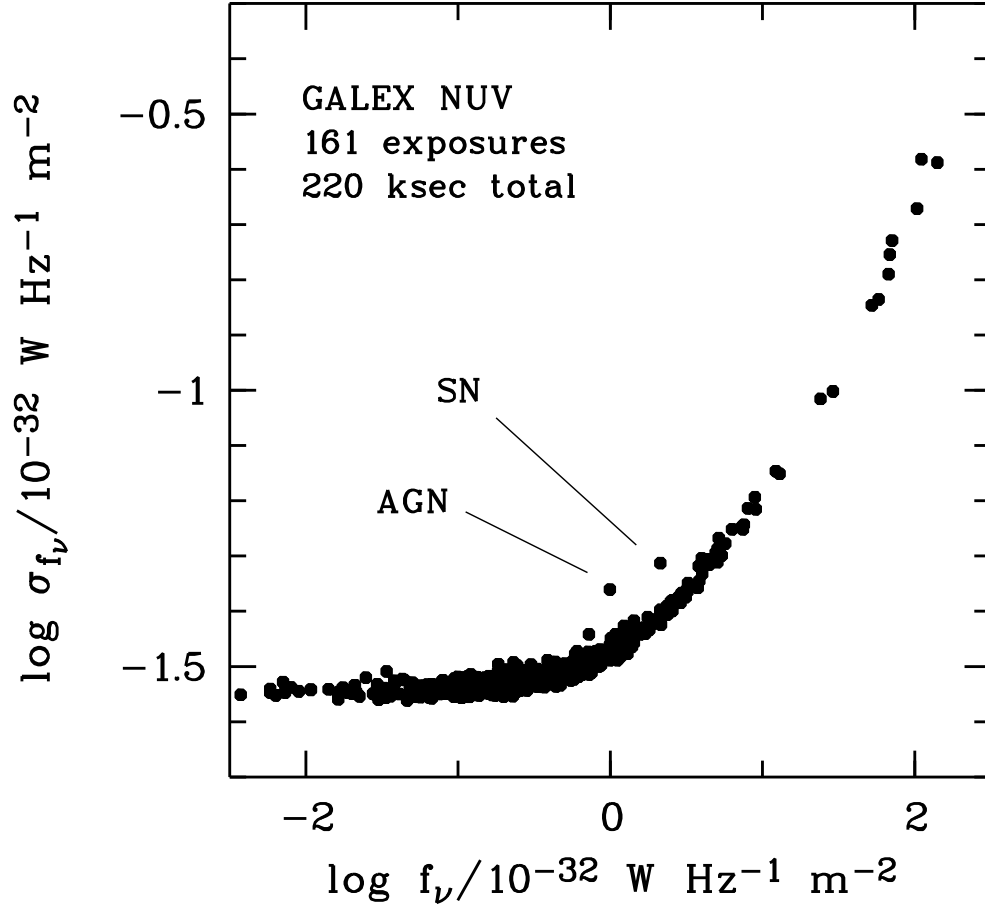


Fig. A3. Mean fluxes f_ν determined from 161 individual measurements and scatter σ_{f_ν} among them. Two objects out of ~ 1000 are clearly variable as evidenced by their increased scatter, one of which is the SN.